

Biogenic Silver Nanoparticles by *Pseudomonas aeruginosa* Reduce Expression of Biofilm and Quorum Signaling Genes in Multi-drug Resistant *Acinetobacter baumannii*

Talar Ibrahim Hasan & Akhter Ahmed Ahmed*

Department of Biology, College of Science, Salahaddin University- Erbil, Iraq

Received: December 30, 2022; Revised: March 1, 2023; Accepted: April 4 2023

Abstract

Discovery of antibiotics is regarded as one of the critical moments in the history of medicine; however, irrational use caused the emergence of a phenomenon known as drug resistance. Once considered benign, *Acinetobacter baumannii* (*A. baumannii*) evolved to become a challenging pathogen threatening the current antibiotic era. In 2017, WHO appointed *A. baumannii* as the most critical pathogen towards which the development of novel antibiotics is keenly required. The current study intends to explore the silver nanoparticles (AgNPs) role in the weakening of virulence and biofilm through reducing the expression of outer membrane protein-A (*OmpA*), biofilm-associated protein (*Bap*), *Acinetobacter baumannii* autoinducer-I (*abaI*) and *Acinetobacter baumannii* receptor (*abaR*) genes in the multi-drug resistant (MDR) *A. baumannii*. All bacterial isolates were capable to form biofilm and exhibited high resistance levels to the antibiotics used including (ampicillin/sulbactam, ceftazidime, tobramycin, amikacin, gentamicin, levofloxacin, imipenem, ciprofloxacin, meropenem, piperacillin/tazobactam, cefepime, ceftriaxone, doxycycline, and trimethoprim/sulfamethoxazole). AgNPs were biologically synthesized by *Pseudomonas aeruginosa* (*P. aeruginosa*) (PA-AgNP) and characterized via FTIR, UV-vis, EDX, XRD, and SEM. Results of characterization tools supported the successful formation of crystalline AgNPs. Minimum-inhibitory concentrations of the harvested AgNPs were determined to study their antibiofilm and quorum quenching potential at sub-inhibitory concentrations (SIC). RT PCR was utilized to estimate the influence of PA-AgNPs on the quorum sensing (QS) and biofilm at level of gene expression. Exposure of the tested isolates to PA-AgNP at SIC values decreased their biofilm fabrication capacity and significantly downregulated candidate genes expression. The results show that *P. aeruginosa* can be used to bio-fabricate AgNPs capable of interrupting bacterial-growth and biofilm progress in the MDR *A. baumannii* through the downregulation of QS and biofilm-associated genes.

Keywords: Quorum sensing, biofilm, virulence, silver nanoparticle, *Acinetobacter baumannii*

1. Introduction

Last century witnessed the revelation of antibiotics which is regarded as one of the most prominent inventions in the history of medicine (Ghosh *et al.*, 2020). For more than 70 years later, antibiotics enabled the treatment of previously lethal bacterial infections and saved millions of lives (Uddin *et al.*, 2021; Laws *et al.*, 2019, Ventola, 2015). However, prolonged overuse and misuse of antibiotics, ineffective infection control strategies, and lack of new drug development have led to the occurrence of a phenomenon known as antibiotic resistance (Aslam *et al.*, 2021; Ventola, 2015). According to a report issued by World Health Organization (WHO) in 2019, antimicrobial resistance was deemed to be responsible for the annual death of at least 700,000 people worldwide and that figure is expected to increase up to 10 million by 2050 if the current situation is left untreated (Nji *et al.*, 2021). As over 70% of the pathogenic bacteria are currently resistant to at least one type of antibiotics, novel approaches should be considered to tackle this global crisis (Uddin *et al.*, 2021;

Laws *et al.*, 2019). Bacteriophages or phage-derived proteins, organic or inorganic nanomaterials in particular gold and silver nanoparticles, probiotics, antimicrobial peptides, repurposing drugs and combination therapy, quorum quenching, and anti-biofilm development are investigated extensively to be used as a possible alternative strategy against superbug infections (García-Contreras *et al.*, 2022).

Acinetobacter baumannii (*A. baumannii*) is an ESCAPE pathogen of great concern regarding both hospital and community-acquired infections and accounts for up to 20% of infections in ICUs globally (Lee *et al.*, 2017). Estimated number of the infectious cases range from 600,000 up to 1,400,000 cases per year throughout the world with fatality rates varying from 20-80% (Havenga *et al.*, 2022). *A. baumannii* is considered the most critical pathogen in the first ever antibiotic resistant priority pathogen list published by WHO in 2017 (Mancuso *et al.*, 2021). Furthermore, disease control and prevention center (CDC) also declared *A. baumannii* as the most urgent in its 2019 antibiotic resistance threat report (CDC, 2019). What makes this pathogen dreadful is a

* Corresponding author. e-mail: akhter.ahmed@su.edu.krd.

repertoire of virulence factors and immense aptitude to withstand stressful environmental settings and multiple classes of antibiotics including “carbapenem” (Ayoub Moubareck and Hammoudi Halat, 2020). Formation of biofilm and virulence factors are sustained by quorum sensing (QS) (Saipriya *et al.*, 2020). Many bacteria use QS as a communication mechanism among each other to sustain population density via production of small diffusible signal-molecules termed autoinducers (Tang *et al.*, 2020; Saipriya *et al.*, 2020).

QS is employed by both gram-positive and gram-negative bacteria where oligopeptides in gram-positive bacteria and acyl-homoserine lactones (AHLs) in gram-negative bacteria are used as the primary autoinducers (Papenfort and Bassler, 2016). Concentration of signaling molecules increases in parallel with the increase in number of bacterial cells, and once a certain threshold has been reached a cascade of reactions will be triggered in response to the binding of autoinducers to their cognate receptors which in turn changes the expression of QS target genes in the bacterial cell (Saipriya *et al.*, 2020; Tang *et al.*, 2020). Recently, a number of reports indicated that two components *Acinetobacter baumannii* autoinducer-I (*abaI*), *Acinetobacter baumannii* receptor (*abaR*) make up the QS regulatory system of *A. baumannii* where the *abaI* is the AHL synthase with 3-hydroxy-C12 homoserine being the primary AHL synthesized and *abaR* is the transcriptional regulator that functions as a receptor for the signal molecules (Cui *et al.*, 2022; Tang *et al.*, 2020). A complex will be formed upon binding of AHL and *abaR* receptor, which in turn attaches to the specific promoter-sequence of the respective genes and modulate their expression (Cui *et al.*, 2022). Quorum quenching refers to various methods used to combat quorum sensing (Ibrahim *et al.*, 2021). Over years a number of synthetic and natural quorum sensing inhibitors have been suggested (Saipriya *et al.*, 2020). Nowadays, the production of nanomaterials has increased (Kumar *et al.*, 2020) and recent developments in nanotechnology made it easier to find use cases for the technology in medicine, electronics, agricultural, renewable energy, and other fields (Pavani *et al.*, 2020). Nanomedicine managed to receive a great deal of recognition from scientists as a possible approach for the drug resistance catastrophe (Uddin *et al.*, 2021). Large amounts of nanoparticles can be manufactured via conventional physical or chemical routes; however, these methods are complicated, expensive, non-ecofriendly, energy-consuming, and require the use of toxic chemicals which limits their biomedical applications (Busi and Rajkumari, 2019). Hence, green-approach for the synthesis of nanoparticles continues to attract more attention because it is simple, requires less energy, cost-efficient, eco-friendly, and is nontoxic (Ball *et al.*, 2019). Among the biological routes, bacteria are considered the best candidate due to their abundance, adaptability, and impressive ability to reduce heavy metal-ions viz, (*Bacillus cereus*, *Pseudomonas stutzeri*, *Bacillus subtilis* and *Pseudomonas aeruginosa*) (Busi and Rajkumari, 2019; Irvani, 2014). Green-synthesized silver nanoparticles targeting bacterial quorum sensing and biofilms are being reported as a novel approach against drug-resistant bacteria (Zhong and He, 2021; Shah *et al.*, 2019). Despite the availability of multiple studies devoted to the effect of inhibitors on *A. baumannii* growth (Raorane *et al.*, 2020;

Singh *et al.*, 2018), none of them has investigated the effect on the level of QS and virulence-related gene expression.

To investigate the role of biogenic silver nanoparticles (AgNPs) in the weakening of QS related virulence and biofilm of the MDR *A. baumannii* through reducing the expression of outer membrane protein-A (*OmpA*), biofilm-associated protein (*Bap*), *abaI* and *abaR* genes, this study was executed.

2. 2. Materials and Methods

2.1. Sample collection and *Acinetobacter baumannii* (*A. baumannii*) identification

This study was conducted in accordance with the principles of the Helsinki Declaration and was approved by the Human Ethics Committee of the Science College at Salahaddin University Erbil (No:4S/478; date, September 9, 2021; Erbil, Iraq).

A total of 26 *A. baumannii* isolates were collected from various bacteriology laboratories of hospitals in the city of Erbil, Kurdistan Region, Iraq. An ATCC strain of *A. baumannii* (19606) was purchased from Medya Diagnostic center to be used as control throughout the study. The clinical isolates were recultivated onto MacConkey (MA, Merck, Germany) agar petri-plates and subjected to aerobic incubation overnight at 37°C. Based on previously described standard techniques in (Tille, 2021), a series of biochemical and conventional diagnostic assays were carried out to establish identification of the individual colonies as *A. baumannii*. Automated Vitek-2 (Biomerieux, France) was employed to validate the identification process. Pure cultures were periodically cultivated on Muller Hinton agar slants and stored at -70°C in nutrient broth supplemented with 25% glycerol for further study.

2.2. Antibiotic susceptibility assay

Guidelines provided by Clinical and Laboratory Institute (CLSI) were considered in the selection of antimicrobial agents to evaluate the sensitivity or susceptibility of the bacterial isolates through disc-diffusion technique (CLSI, 2022). Prior to inoculation onto the Muller Hinton agar (MHA, Biomark Laboratories, India) plates, turbidity or clarity of the bacterial suspensions was accommodated to 0.5 McFarland by a spectrophotometer. Following lawn plating, the plates were then subjected to the following antibiotics: ampicillin/sulbactam (10/10 µg, Himedia), ceftazidime (30 µg, Bioanalyse), tobramycin (10 µg, Bioanalyse), amikacin (10 µg, Bioanalyse), gentamicin (10 µg, Bioanalyse), levofloxacin (5 µg, Bioanalyse), imipenem (10 µg, Bioanalyse), ciprofloxacin (10 µg, Bioanalyse), meropenem (10 µg, Bioanalyse), piperacillin/tazobactam (100/10 µg, Himedia), cefepime (10 µg, Bioanalyse), ceftriaxone (10 µg, Bioanalyse), doxycycline (10 µg, Bioanalyse), and trimethoprim/sulfamethoxazole (25 µg, Himedia).

For data analysis, The CLSI diameter breakpoints shown in table (1) were employed, and data were interpreted as susceptible, intermediate and resistant. The most resistant strains were selected to test the inhibitory effect of PA-AgNPs. Two biological replicates were considered on different occasions.

Table 1. Antibiotic inhibition zone interpretive standard for *A. baumannii* according to clinical and laboratory institute

Antibiotic Agents	Code	Inhibition Zone Diameter (mm)		
		Sensitive	Intermediate	Resistant
Amikacin	AK	≥17	15-16	≤14
Ampicillin – Sulbactam	A/S	≥15	12-14	≤11
Cefepime	CEF	≥18	15-17	≤14
Ceftazidime	CAZ	≥18	15-17	≤14
Ceftriaxone	CRO	≥21	14-20	≤13
Ciprofloxacin	CIP	≥21	16-20	≤15
Doxycycline	DO	≥13	10-12	≤9
Gentamicin	GEN	≥15	13=14	≤12
Imipenem	IPM	≥22	19-21	≤18
Levofloxacin	LEV	≥17	14-16	≤13
Meropenem	MER	≥18	15-17	≤14
Piperacillin – Tazobactam	P/T	≥21	18-20	≤17
Tobramycin	TOB	≥15	13-14	≤12
Trimethoprim - sulfamethoxazole	T/S	≥16	11-15	≤10

2.3. Static biofilm assay

The microplate technique described by (Limban *et al.*, 2011) was adopted with slight modifications to examine the ability of the identified *A. baumannii* isolates to form biofilm. In brief, 15 µl of the overnight cultures of the desired bacteria were inoculated into wells of the microtiter plate (MTP, Citotest Labware, China) containing 200 µl of sterile Nutrient broth (NB, Neogen, USA) supplemented with 2% glucose. Wells containing NB only served as control. Then, the inoculated MTP was incubated for 24 hours in a static condition at 37°C. Following the incubation period, the cavities were rinsed thrice with sterile phosphate buffer saline (PBS) after disposal of the supernatant. The wells were dried at 55°C by oven (memmert, Germany), 200 µl of 1% crystal-violet staining solution was allocated into each of the cavities and incubated for (10 minutes) at ambient temperature. Lastly, the wells of the microplate were carefully rinsed thrice with sterilized PBS and eluted with 95% ethanol solvent to quantify the biofilms produced spectrophotometrically by mean of ELISA (BioTek Instruments, USA) at a wavelength of 490 nm. Three biological replicates were considered on different occasions.

2.4. Bio-fabrication of biogenic silver nanoparticles

The method described by (Nirmala and Sridevi, 2021) with slight modifications was employed for the bio-fabrication of PA-AgNPs by an ATCC strain of *Pseudomonas aeruginosa* (*P. aeruginosa*) (50126). First, a loopful of the *P. aeruginosa* inoculum was placed in 500 ml of sterile NB and incubated overnight at 37°C. Following incubation, the broth was centrifuged for 10 minutes at 6000 rpm to obtain a cell-free broth. The later was mixed with 500 ml of 4 mM silver-nitrate and incubated in the dark for 72 hours at 60°C. After the incubation period, a transition in the color of the reaction-mixture to dark brown was regarded as the initial indicator for AgNPs synthesis. The stronger biofilm producers were selected to test the antibacterial effect of PA-AgNPs.

Three biological replicates were considered, and standard errors were measured.

2.5. Characterization of biogenic silver nanoparticles

The existence of the formed PA-AgNPs was confirmed via using Ultraviolet-visible spectroscopy (UV-1900i, Shimadzu, Japan). Energy-Dispersive X-Ray analysis (EDS), Scanning-Electron Microscopy (SEM), X-ray Diffraction (XRD), and Fourier-Transform Infrared-Spectroscopy (FTIR) (Jasco, Japan) were employed to further characterize the harvested PA-AgNPs (Nirmala and Sridevi, 2021).

2.6. Minimum and sub-minimum inhibitory concentration (MIC and SIC) determination of PA-AgNPs

CLSI instructions were utilized accordingly to assess MIC of the prepared PA-AgNPs against ten of the clinical MDR and the most frequent biofilm producers along with an *A. baumannii* ATCC 19606 through broth-microdilution technique (CLSI, 2018). 200µL NB containing different concentrations (80, 40, 20, 10, 5, 2.5, 1.25 mg/ml) of PA-AgNPs were administered to the wells of MTP. Then 10 µl of overnight *A. baumannii* culture adjusted to the standard 0.5 McFarland was added to the wells and incubated overnight aerobically in the rotating incubator (150 rpm) at 37°C. The wells with no evident growth were determined as MIC. SIC values were ruled as the measures below the MIC values and were employed to appraise anti-biofilm/anti-QS activity of the PA-AgNPs.

2.7. SIC effect of PA-AgNPs on the biofilm

The protocol described by (Ahmed and Salih, 2019) was considered to evaluate the impact of the PA-AgNPs on biofilm fabrication by the ten clinical MDR and strongest strains along with an *A. baumannii* ATCC 19606 at SIC. Briefly, 15 µl from the sub-MICs wells of the previous procedure (MIC) were allocated into wells of flat-bottom MTP containing 200 µl of nutrient broth supplemented with 2% glucose. Then, the inoculated MTP was placed in the incubator at 37°C for 24 hours under a static condition. Wells containing NB with bacterium inoculum only used as control. Following the incubation period, 1% crystal-violet was applied to stain the microplate after disposal of the liquid-cultures from the wells and rinsing with PBS thrice. After the staining procedure, the wells were rinsed with PBS, eluted with 95% ethanol, and subjected to ELISA in order to quantify the biofilm produced at the wavelength of 490 nm.

2.8. RNA extraction and quantification of QS and biofilm related genes

Real-time PCR instrument (RT-PCR) was operated to assess the PA-AgNPs effect at the SIC value on the expression extent of the outer membrane protein-A (*OmpA*), biofilm-associated protein (*Bap*), *Acinetobacter baumannii* autoinducer-I (*abaI*) and *Acinetobacter baumannii* receptor (*abaR*) genes. Total RNA was extracted from both untreated bacteria which were used as control and bacteria exposed to PA-AgNPs following guidance provided by the manufacturer (total RNA kit, Favorgen Biotech, Taiwan). cDNA was synthesized through reverse transcription of the isolated RNA using the AddScript cDNA synthesis kit coinciding with the manufacturer protocol (addbio, Korea). RT-PCR reactions

were executed utilizing “RealQ-Plus 2x Master-Mix Green” (Ampliqon, Denmark) in the PCRmax Eco 48 RT-PCR system. Primer sequences listed in Table (2) were

used to analyze candidate genes via (RT-PCR) and the procured results were calculated using the $\Delta\Delta C_t$ method (Ahmed and Salih, 2019).

Table 2. List of genes and their primer sequences

Gene	Primer Sequence (5'-3')		Product size(bp)	Ref.
	Forward	Reverse		
<i>abaI</i>	AAAGTTACCGCTACAGGG	CACGATGGGCACGAAA	435	(Tang <i>et al.</i> , 2020)
<i>abaR</i>	TCCTCGGGT CCCAATA	AAATCTACCGCATCAA	310	(Tang <i>et al.</i> , 2020)
<i>ompA</i>	ATGAAAAAGACAGCTATCGCGATTGCA	CACCAAAAAGCACCCAGCGCCAGTTG	136	(Amin <i>et al.</i> , 2019)
<i>Bap</i>	AATGCACCGGTACTTGATCC	TATTGCCTGCAGGGTCAGTT	205	(Amin <i>et al.</i> , 2019)

2.9. Statistical analysis

The obtained results were analyzed through GraphPad Prism 8.0 software. Two-way analysis of variance (ANOVA) method was selected for multiple comparisons. Data presented as mean \pm SE.

3. Results

3.1. *Acinetobacter baumannii* (*A. baumannii*) isolates

A total of 27 *A. baumannii* isolates including ATCC (19606) were obtained from various hospitals in Erbil governorate to conduct the current study. The bacterial isolates were identified as gram-negative coccobacilli, catalase-positive, oxidase-negative, indole-negative, citrate-positive, non-fermentative bacteria capable of growth on MacConkey agar. To confirm their identification, Vitek-2 system was employed to identify the isolates as *A. baumannii* with a probability rate of 96 to 99%. Following specimen type analysis, it was found that (58%) of the clinical isolates were recovered from sputum followed by wound (27%), blood (12%), and CSF (4%) as seen in figure (1).

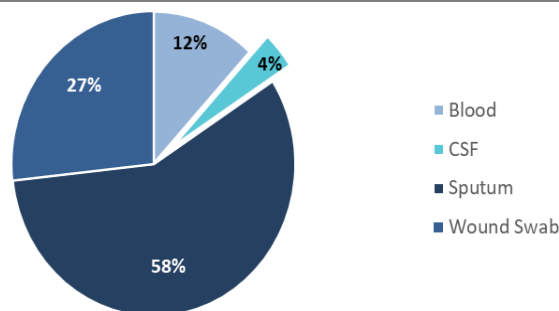


Figure 1. Different clinical specimens recovered from patients with *A. baumannii* including sputum, wound, blood, and CSF

3.2. Antibiotic sensitivity pattern

Kirby-Bauer test was employed to evaluate the susceptibility of the isolates to the antibiotics included in this study and the results indicated that all isolates showed 100% resistance to cefepime and ceftazidime followed by 96% resistance to amikacin, 93% resistance to (ceftriaxone, ciprofloxacin, gentamicin, levofloxacin), 78% imipenem, 74% meropenem, 70% doxycycline, 67% tobramycin, 63% trimethoprim/sulfamethoxazole, 33% piperacillin/tazobactam and least resistance was shown to ampicillin/sulbactam with a percentage of only 26% as shown in figure (2).

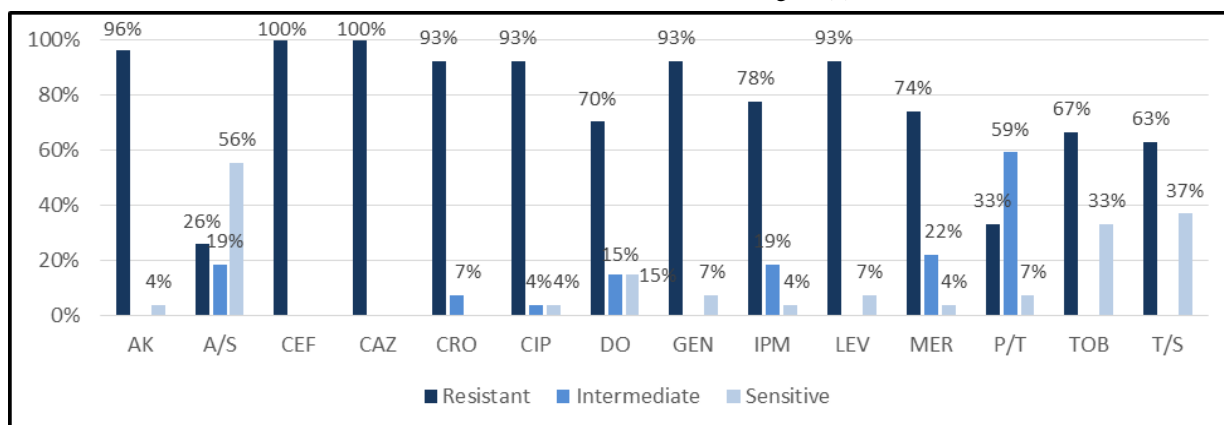


Figure 2. Percentage of sensitive, intermediate, and resistant *A. baumannii* isolates obtained from antibiotic sensitivity assay: AK (Amikacin); A/S (ampicillin/sulbactam); CEF (cefepime); CAZ (ceftazidime); CRO (ceftriaxone); CIP (ciprofloxacin); DO (doxycycline); GEN (gentamicin); IPM (imipenem); LEV (levofloxacin); MER (meropenem); P/T (piperacillin/tazobactam); TOB (tobramycin); T/S (trimethoprim/sulfamethoxazole).

Furthermore, based on the antibiotic susceptibility test results *A. baumannii* isolates were categorized into three groups (MDR, XDR, and non-MDR). It was calculated that the majority of isolates were XDR with a whopping percentage of 67%, 30% were MDR and around 4% were observed to be non-MDR as illustrated in figure (3).

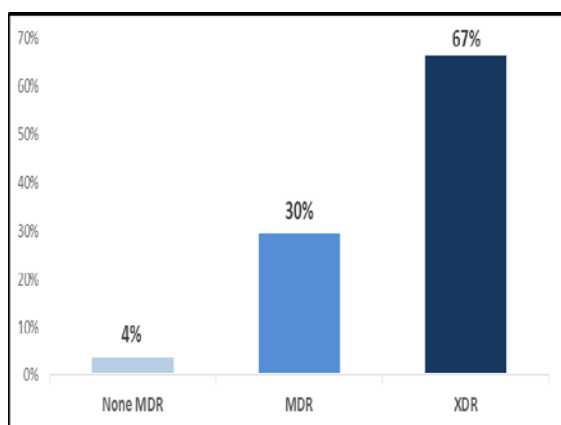


Figure 3. Distribution of *A. baumannii* isolates according to their pattern of resistance

3.3. Biofilm analysis

The microplate method was considered to evaluate capability of the *A. baumannii* strains to form biofilms. Results indicated that while 11% of the strains were marked as potent biofilm producers, 48% and 41% were labeled as moderate and weak biofilm formers as presented in figure (4).

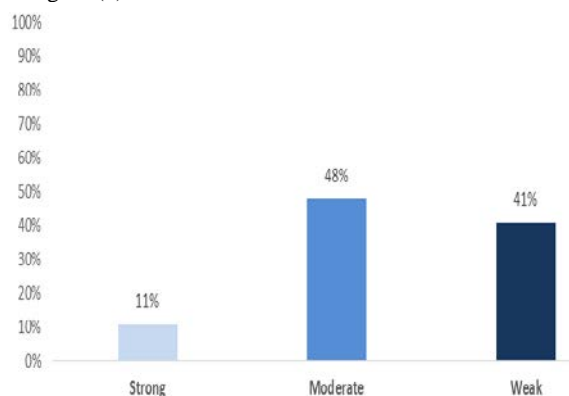


Figure 4. Percentage of the biofilm development status of isolates based on results obtained from the microtiter plate method.

3.4. Biosynthesis and characterization of nano-silvers

The standard strain of *Pseudomonas aeruginosa* ATCC 50126 was utilized to manufacture the AgNPs biologically. Following incubation at 60 °C for 72 hours, a switch in the reaction-mixture color from pale yellow to deep brown manifested was viewed as the initial indicator for the presence of nano-silver. UV-vis spectroscopy was employed to confirm the bio-reduction of AgNO₃ to AgNPs. Absorption peak at 268 nm was observed for the silver-nitrate solution solely; however, after 72 hours of incubation with the cell-free supernatant this peak vanished, and a new peak was observed at 420 nm indicating the formation of PA-AgNPs as observed in figure (5).

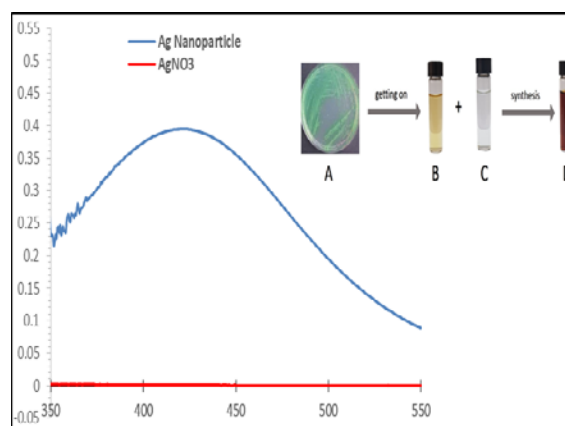


Figure 5. UV-Vis spectrum of bio-fabricated AgNPs and demonstration of AgNPs bio-fabrication: (A) *P. aeruginosa* ATCC 50126; (B) cell-free supernatant; (C) AgNO₃; (D) reduction of silver ion to nanoparticle.

3.5. FTIR analysis

FTIR measurements in the range of 400 to 4000 cm⁻¹ were conducted in order to identify functional groups in the biological compounds that may be implicated in the bio-reduction of AgNO₃, and bio-capping of nano-silver. FTIR spectra of the biosynthesized PA-AgNPs were compared with the standard values to detect functional groups. Hence, obtained bands at 3266, 2136, 1735, 1635, 1369, and 1218 cm⁻¹ were analogous to the O-H (alcohol), C≡C (alkyne), C=O (carbonyl), C double bond (alkene), C-H (alkane) and C-O for (carboxylic acids, ethers, alcohols, esters) stretching vibrations (Figure 6).

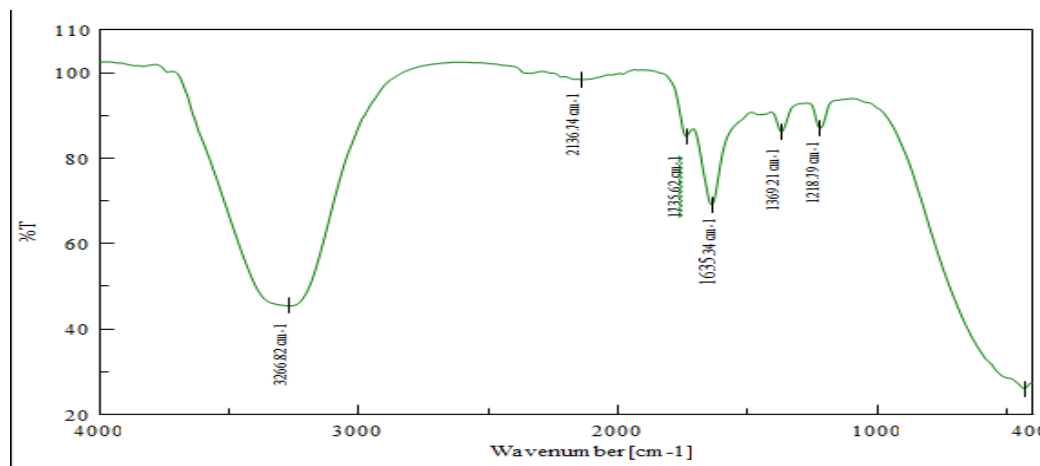


Figure 6. FTIR spectra of *P. aeruginosa* synthesized silver nanoparticles.

3.6. XRD

Crystal-like nature of the PA-AgNPs was confirmed via XRD analysis. Figure (7) represents XRD pattern of our sample which shows 8 distinct peaks at 2θ of 27.219, 31.674, 45.707, 54.333, 56.954, 66.941, 74.025 and 76.242 corresponding to 111, 200, 311, 222, 400, 331, 420 and 422 planes of face-centered-cubic silver nanoparticles respectively. These findings were further supported by the international center for diffraction data (JCPDS no. 98-005-6538). The Debye-Scherrer formula was employed to calculate crystallite size from the XRD data, and the average crystallite size was 28.32nm.

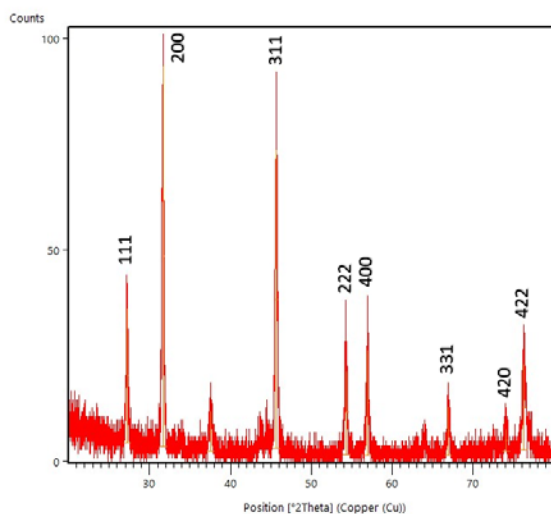


Figure 7. XRD spectra of biosynthesized silver nanoparticle.

3.7. SEM and EDAX

SEM instrument was utilized to study the surface morphology and size of PA-AgNPs which appeared to be spherically shaped and polydispersed with a size range of 45nm to 50 nm (Figure 8).

Furthermore, EDAX was operated to inspect the elemental makeup of the bio-fabricated PA-AgNPs. From figure (9), we can observe an intense absorption peak at 3 KeV suggesting the presence of metallic AgNPs. In addition to silver, we can also observe chlorine peak. Total weight of the element silver was found to be 84.15% whereas chlorine was 15.85%.

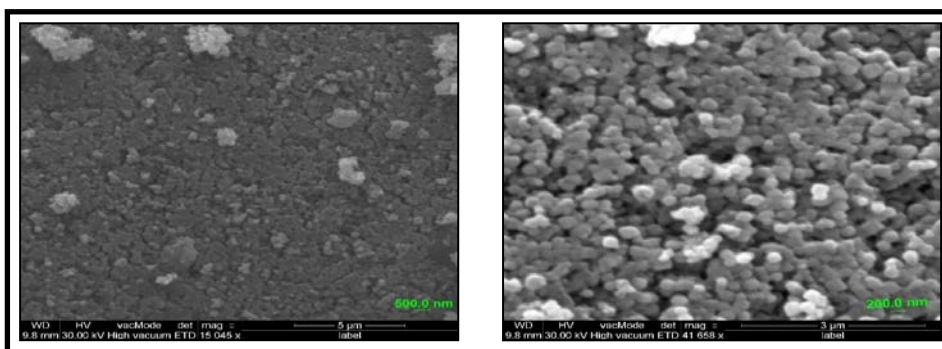


Figure 8. SEM micrograph of biosynthesized PA-AgNPs.

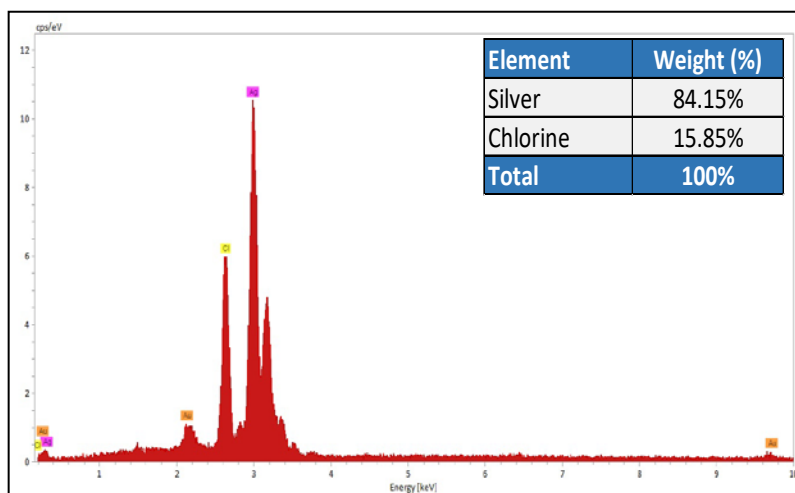


Figure 9. EDAX profile of green synthesized AgNPs.

3.8. Effect of biogenic silver nanoparticle on the isolates at SIC

To analyze antibiofilm potential of the bacteriogenic nano-silvers in the tested isolates at SIC, we first needed to unveil the MIC values of the bio-fabricated AgNPs via broth-microdilution technique. For this purpose, 10 of the strongest biofilm-producing isolates along with an ATCC strain were employed and the results showed MIC values between 10 to 20 mg/ml along with respective SIC values of 5 to 10 mg/ml as detailed in table (3).

Table 3. Minimum-inhibitory concentrations (MICs) and Sub-MICs of biogenic PA-AgNPs of MDR *A. baumannii*.

Bacterial isolates	MIC (mg/ml)	Sub-MIC (mg/ml)
3	10	5
5	20	10
6	20	10
11	20	10
13	20	10
14	10	5
16	10	5
20	20	10
21	20	10
23	20	10
ATCC (19606)	20	10

The influence of the bio-formulated AgNPs on the capacity of the selected strains to develop biofilm at SIC values was elucidated via microplate protocol, and the results indicated that exposure to the PA-AgNPs significantly ($P < 0.0001$) lowered biofilm production in all of the selected isolates as observed in figure (10).

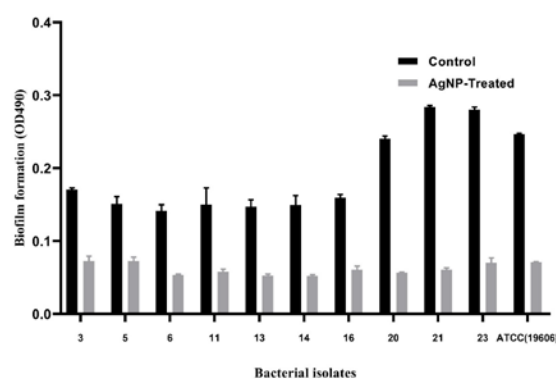


Figure 10. Quantitative measurement of *Acinetobacter baumannii* biofilm reduction by SIC of biogenic PA-AgNPs. Data are displayed as (mean±SE). All data are significant at $P < 0.0001$.

3.9. Impact of PA-AgNPs on biofilm and virulence related gene expression of *A. baumannii*

The level of gene-expression for each of the candidate genes was evaluated in the selected isolates in the presence and absence of PA-AgNPs using qPCR. Following analysis of the obtained results, we indicated that PA-AgNPs affected the tested isolates differently as observed in figure (11). The expression level of all candidate genes in samples A2 and A3 were down-regulated significantly following exposure to PA-AgNPs. However, the *Bap* gene was not affected in sample A1. Interestingly, neither QS genes nor *OmpA* gene were down-regulated in the ATCC sample treated with PA-AgNPs.

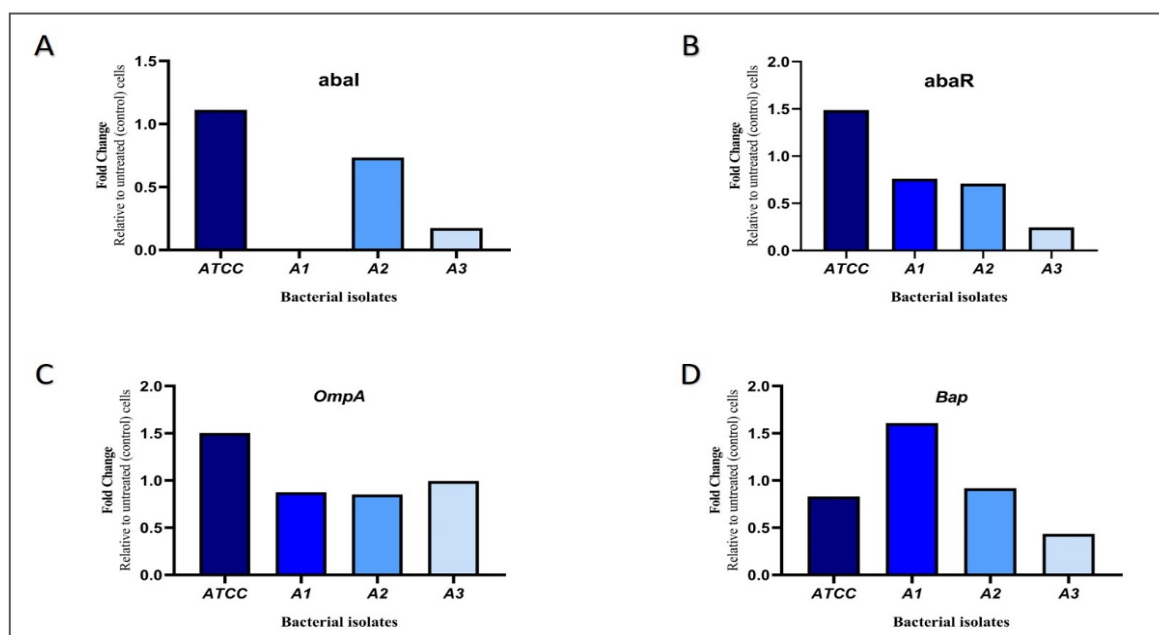


Figure 11. Fold change in the expression level of candidate genes (*abaI*, *abaR*, *OmpA*, *Bap*) in the treated bacterial isolates relative to untreated control cells.

4. Discussion

Currently, drug resistance is regarded as a major problem posing threat to not just global health but also to development and food security (Nji *et al.*, 2021). *Acinetobacter baumannii* (*A. baumannii*) is equipped with a repertoire of virulence factors that enable the bacteria to cause a series of life-threatening infections and resist stressful environmental circumstances (Ayoub Moubareck and Hammoudi Halat, 2020). They can cause infections in various sites in the body such as urinary-tract infections, wound infections, pneumonia, meningitis, and septicemia (Hetta *et al.*, 2021; Ayoub Moubareck and Hammoudi Halat, 2020). In the current study, we collected 26 clinical isolates in which the majority were recovered from sputum followed by wound, blood, and CSF specimens as observed in figure (1). Similarly in a recent study from Iraq 38 *A. baumannii* isolates were collected out of which 32% were recovered from sputum followed by 29% swabs, 21% urine, 13% blood, and 5% fluid (Muhsin *et al.*, 2022). The reason for the isolation of the bacteria from sputum at a higher percentage could be due to the tendency of the pathogen to infect the respiratory-tract most commonly (Li *et al.*, 2017). Various adhesins and the ability to develop biofilm participate greatly in their pathogenesis and resistance to antibiotics (Ghasemian *et al.*, 2019). Also, it is well-known that the bacteria living in biofilm are able to resist antibiotics 1000 fold higher than the free-living or planktonic bacteria, which in turn minimizes our choices for an effective antibiotic therapy (Hall and Mah, 2017). In this regard, all of our isolates produced biofilm and showed resistance to the tested antibiotics at varying degrees. Forty-eight percentage of our isolates were recorded as moderate biofilm producers while 11% and 41% were strong and weak biofilm producers as illustrated in figure (4). These observations agree with the findings of another study in which 100% of the isolates produced biofilm and the majority were reported to be moderate biofilm producers (Sherif *et al.*, 2021). In the present

study, 67% of the strains were categorized as XDR as seen in figure (3). A similar resistance pattern was reported by Maspi *et al* where 71.2% of the confirmed *A. baumannii* isolates were XDR (Maspi *et al.*, 2016). Among the 14 tested antibiotics, highest level of resistance was observed against cefepime and ceftazidime where all isolates exhibited 100% resistance followed by 96% to amikacin and maximum susceptibility (56%) was shown against ampicillin/sulbactam as seen in figure (2). Our antibiotic susceptibility results are in line with a study from Tehran that reported the isolates to be resistant to majority of antibiotics including 100% resistance to cefepime and ceftazidime along with 90% resistance to amikacin (Khoshnood *et al.*, 2017). WHO has appointed *A. baumannii* as the most critical pathogen towards which investigation, discovery and development of new antibiotics are eagerly required (Ayoub Moubareck and Hammoudi Halat, 2020). In this regard, a number of reports have been issued in the last few decades highlighting the successful use of nanoparticles in particular AgNPs as an effective antibacterial agent (Kaur *et al.*, 2021). Compared to other nanoparticles, AgNPs are less toxic and are more effective in combating microorganisms; hence, they are studied more extensively and are viewed as the upcoming antibiotic generation. AgNPs are cytotoxic to microbes due to their ability to increase cell permeability by damaging both cell wall and cell membrane and cause internal damage through release of silver-ions that trigger oxidative stress and cell death through production of reactive-oxygen and interfering with vital processes of the cell (Mba and Nweze, 2021).

Bacteria synthesize biogenic nanoparticles either intracellularly or extracellularly in the presence of enzymes; however, extracellular production does not require added purification steps and is considered more cost-efficient (Nirmala and Sridevi, 2021). C-type cytochromes, reducing-cofactors, Ag-resistant genes,

peptides, and enzymes such as nitrate reductase empower the bacteria to reduce and stabilize silver ions to AgNPs (Singh *et al.*, 2015). In this aspect, studies were conducted by Oza *et al.* (2012) and Paul and Sinha (2014) where *Pseudomonas aeruginosa* (*P. aeruginosa*) was successfully used to synthesize well-dispersed AgNPs. In another part of the study, they confirmed the involvement of nitrate reductase as the reducing agent. Furthermore, Peiris and coworkers conducted a research where they compared the antimicrobial effect of nano-silvers synthesized by each of “*Escherichia coli*, *A. baumannii*, *Staphylococcus aureus*, *P. aeruginosa*” and they indicated most stable AgNPs were bio-fabricated by *P. aeruginosa* that showed broad antimicrobial effect (Peiris *et al.*, 2018). Consequently, we chose *P. aeruginosa* for extracellular synthesis of AgNPs. From figure (5), we can observe the shade of the reaction-mixture swapped from pale yellow to dark brown following incubation which is thought to be due to a phenomena known as surface plasmon resonance and is regarded as an initial indicator for reduction of Ag-ion to nanoparticles (Nirmala and Sridevi, 2021). Occurrence of this characteristic brown color has also been reported previously by (Sunkar and Nachiyar, 2012). Spherically-shaped AgNPs with sizes ranging from 2 to 100 nm would be expected in case a single UV spectral band between 410 and 440 nm was observed (Haji *et al.*, 2022). In our study, we observed a single UV band at 420nm for our PA-AgNPs suggesting that our particles were spherical and parallel to SEM images. Similar observations were made by (Bhatt *et al.*, 2018) where they reported a single UV peak at 430 nm using cell free extract of *P. aeruginosa*. SEM observations indicate that our nanoparticles are uniform, spherical with little to no aggregation and size was ranged from 45 to 50 nm (Figure 8). Our findings reveal smaller particle sizes and better dispersity compared to (Peiris *et al.*, 2017) where majority of nanoparticles had size range of 50 to 100nm. Elemental-composition of the PA-AgNPs was investigated via EDX where we noticed intense absorption peak for silver at 3 Kev confirming formation of AgNPs (Ibrahim *et al.*, 2019). The results of EDX indicate higher distribution of silver element with a percentage of 84.15% in the green PA-AgNPs as demonstrated in figure (9). Presence of chlorine could be due to emissions from enzymes or proteins in the culture-supernatant (Kumar and Mamidyala, 2011). In agreement with our results, intense absorption peak at 3 Kev was observed by EDX analysis of *Pseudomonas* spp AgNPs (Punjabi *et al.*, 2017). FTIR was used to detect functional groups that could have led to bio-reduction of silver-ions. FTIR results seen in figure (6) revealed 6 peaks at 3266, 2136, 1735, 1635, 1369 and 1218 cm^{-1} parallel to O-H (alcohol), C=C (alkyne), C=O (carbonyl), C double bond (alkene), C-H (alkane) and C-O for (carboxylic acids, ethers, alcohols, esters) stretching vibrations (Bhatt *et al.*, 2018). Overall, FTIR analysis indicated presence of a number of biomolecules that might have reduced and capped the green PA-AgNPs (Yang *et al.*, 2020). Fernando *et al.* also revealed presence of carbonyl and alkene groups following FTIR spectrum analysis of AgNPs synthesized by means of *P. aeruginosa* indicating stabilization of the nanoparticles with aid of proteins (Peiris *et al.*, 2017). In accordance with standard data, XRD analysis confirmed PA-AgNPs to be face-centered-cubic crystals. According to Ahmed *et al.*,

(2020), the intense labeled peaks observed in figure (7) are thought to be brought about by capping agents that stabilized the nanoparticle. In a recent study, XRD was also used to confirm AgNPs Crystalline nature synthesized by a *P. aeruginosa* strain (Yang *et al.*, 2020). Based on XRD data profile we ascertained average crystallite size of 28.32 nm using Scherer formula ($D=K\lambda/\beta hkl\cos\theta$) (Bindu and Thomas, 2014). Average crystallite size in this study was much smaller compared to a previous report that made use of Scherer formula to calculate crystallite size (Abootalebi *et al.*, 2021).

Recently, numerous studies delineated the antimicrobial effect of nanosized silver (Urnukhsaikhan *et al.*, 2021; Ali *et al.*, 2020). However, studies regarding the inhibitory impact of silver-based nanoparticles bio-fabricated by bacteria on biofilm formation and quorum signaling (QS) are scarce. The expression of numerous virulence factors is under the control of QS; hence, any interference with this system can lead to the downregulation of the virulence genes (Zhong and He, 2021).

Our results showed the antibiofilm ability of silver where SIC of PA-AgNPs greatly decreased the competency of the tested strains to construct biofilms as shown in figure (10). Accordant with our results, earlier reports also emphasized the role of AgNPs as a potent biofilm inhibitor (Slavin *et al.*, 2021). The anti-biofilm and anti-QS effect of our PA-AgNPs were evaluated using relative RT-PCR. We observed that exposure of the tested isolates to SIC values of PA-AgNPs greatly affected the expression of the candidate genes as observed in figure (11). A number of genes including *Bap*, *abal*, and *OmpA* are believed to participate in the development of biofilm in *A. baumannii* (Dolma *et al.*, 2022). Downregulation of each of *Bap*, *abal*, and *OmpA* genes may lead to the inhibition of biofilm (Nie *et al.*, 2020; Alejandro *et al.*, 2018). Moreover, a number of reports previously stated a decrease in the ability of the bacteria to develop biofilm following inhibition of *abaR* gene (Sun and Xiang, 2021). Hence, the decline observed in the ability of our clinical isolates to develop biofilm maybe due to disruption in the expression of *Bap*, *OmpA*, and QS genes. Inhibition of QS genes by means of a chemical AgNPs was lately reported in a study (Hetta *et al.*, 2021). However, the current study represents the first report regarding the anti-biofilm/anti-QS effect of green AgNPs synthesized by means of *P. aeruginosa* in opposition to clinical *A. baumannii*. Due to time limitations, economic burden and shortage in the quantity of the nanoparticles, we could not operate transmission electron microscopy (TEM) for our nanoparticles since it needed to be sent abroad; nor could we include more strains to examine the AgNPs effect on level of gene expression.

5. Conclusion

Reinforced by the experimental outcomes of this study, we conclude that *P. aeruginosa* can be used to bio-fabricate AgNPs (PA-AgNPs) in an efficient and cost-effective manner. The majority of our clinical isolates portrayed elevated resistance to the selected antimicrobials and were all competent to construct biofilms at varying degrees. Exposure of the isolates to PA-AgNPs at SIC greatly reduced their ability to form biofilm. Furthermore,

PA-AgNPs treated isolates exhibited pronounced reduction in the level of QS, *OmpA* and *Bap* genes expression which are culpable for the development of resistance and biofilm in *A. baumannii*. Hence, anti-QS anti-biofilm results of the green AgNPs obtained from the current study could pave the way for their use as a promising nanomaterial in the battle against the critical pathogen *A. baumannii* through interfering with their QS mechanism.

Author contribution

AA outlined research; TI & AA conducted research and analyzed data; TI wrote the paper; AA superintended the study and edited the paper. TI & AA read and approved the final version of the manuscript.

Data Availability

The data used to support the findings of this study are included within the article.

Conflict of interest

All authors declared no conflict of interest in the present manuscript.

Funding Statement

No funding.

References

- Abootelebi S, Mousavi SM, Hashemi SA, Shorafa E, Omidifar N & Gholami A. 2021. Antibacterial effect of green synthesized silver nanoparticles using ferula assafoetida against *Acinetobacter baumannii* isolated from the hospital and their cytotoxicity on the human cell line. *J. Nanomater*, **2021**: 1-12.
- Ahmed AA and Salih FA. 2019. Quercus infectoria gall extracts reduce quorum sensing-controlled virulence factors production and biofilm formation in *Pseudomonas aeruginosa* recovered from burn wounds. *BMC Complement Altern Med*, **19** (1): 1-11.
- Ahmed FY, Aly UF, Abd El-Baky RM and Waly NG. 2020. Comparative study of antibacterial effects of titanium dioxide nanoparticles alone and in combination with antibiotics on *mdr Pseudomonas aeruginosa* strains. *Int J Nanomedicine*, **15**: 3393-3404.
- Alejandro H-MD, Humberto M-OM, Fidel G-L, Antonio G-LM and Eduardo S-G. 2018. Inhibition of *Acinetobacter baumannii* biofilm formation by methanolic extract of *nothoscordum bivalve*. *Adv Microbiol*, **8**(5): 422-438.
- Ali Z, Mirani DZ, Urooj S, Khan M, Khan AB, Shaikh I, Siddiqui A and Za M. 2020. An effective weapon against biofilm consortia and small colony variants of MRSA. *Iran J Basic Med Sci*, **23**: 1494-1498.
- Amin M, Navidifar T, Shooshtari FS, Rashno M, Savari M, Jahangirmehr F and Arshadi M. 2019. Association between biofilm formation, structure, and the expression levels of genes related to biofilm formation and biofilm-specific resistance of *Acinetobacter baumannii* strains isolated from burn infection in ahvaz, iran. *Infect Drug Resist*, **12**: 3867-3881.
- Aslam B, Khurshid M, Arshad MI, Muzammil S, Rasool M, Yasmeen N, Shah T, Chaudhry TH, Rasool MH, Shahid A, Xueshan X and Baloch Z. 2021. Antibiotic resistance: One health one world outlook. *Front Cell Infect Microbiol*, **11**: 1-20.
- Ayoub Moubareck C and Hammoudi Halat D. 2020. Insights into *Acinetobacter baumannii*: A review of microbiological, virulence, and resistance traits in a threatening nosocomial pathogen. *Antibiotics (Basel)*, **9**(3): 1-28.
- Ball AS, Patil S and Soni S. 2019. Introduction into nanotechnology and microbiology, *Methods Microbiol*, **46**: 1-18.
- Bhatt D, Gupta E, Kaushik S, Srivastava VK, Saxena J and Jyoti A. 2018. Bio-fabrication of silver nanoparticles by *Pseudomonas aeruginosa*: Optimisation and antibacterial activity against selected waterborne human pathogens. *IET Nanobiotechnol*, **12**(7): 981-986.
- Bindu P and Thomas S. 2014. Estimation of lattice strain in ZnO nanoparticles: X-ray peak profile analysis. *J Theor Appl Phys*, **8**(4): 123-134.
- Busi S and Rajkumari J. 2019. **Microbially synthesized nanoparticles as next generation antimicrobials: Scope and applications**, in *Nanoparticles in Pharmacotherapy*, William Andrew Publishing.
- CDC. 2019. **Antibiotic resistance threats in the United States**. Centers for Disease Control and Prevention. Available: <https://www.cdc.gov/drugresistance/biggest-threats.html>.
- CLSI. 2018. **Methods for dilution antimicrobial susceptibility tests for bacteria that grow aerobically; approved standard. eleventh Edition**. CLSI document M07. Wayne, PA: Clinical and Laboratory Standards Institute.
- CLSI. 2022. **Performance standards for antimicrobial susceptibility testing**. Informational Supplement. CLSI document M100Ed32E. Wayne, PA: Clinical and Laboratory Standards Institute.
- Cui B, Chen X, Guo Q, Song S, Wang M, Liu J and Deng Y. 2022. The cell-cell communication signal indole controls the physiology and interspecies communication of *Acinetobacter baumannii*. *Microbiol Spectr*, **10**(4): 1-12.
- Dolma KG, Khatri R, Paul AK, Rahmatullah M, De Lourdes Pereira M, Wilairatana P, Khandelwal B, Gupta C, Gautam D, Gupta M, Goyal RK, Wiart C and Nissapatorn V. 2022. Virulence characteristics and emerging therapies for biofilm-forming *Acinetobacter baumannii*: A review. *Biology*, **11**(9): 1-20.
- García-Contreras R, Martínez-Vázquez M, González-Pedrajo B and Castillo-Juárez I. 2022. Editorial: Alternatives to combat bacterial infections. *Front Microbiol*, **13**: 1-5.
- Ghasemian A, Mobarez AM, Peerayeh SN and Bezmin Abadi AT. 2019. The association of surface adhesion genes and the biofilm formation among *Klebsiella oxytoca* clinical isolates. *New Microbes New Infect*, **27**: 36-39.
- Ghosh D, Veeraraghavan B, Elangovan R and Vivekanandan P. 2020. Antibiotic resistance and epigenetics: More to it than meets the eye. *Antimicrob Agents Chemother*, **64**(2): 1-27.
- Haji SH, Ali FA and Aka STH. 2022. Synergistic antibacterial activity of silver nanoparticles biosynthesized by carbapenem-resistant gram-negative bacilli. *Sci Rep*, **12**(1): 1-13.
- Hall CW and Mah T-F. 2017. Molecular mechanisms of biofilm-based antibiotic resistance and tolerance in pathogenic bacteria. *FEMS Microbiol Rev*, **41**(3): 276-301.
- Havenga B, Reyneke B, Waso-Reyneke M, Ndlovu T, Khan S and Khan W. 2022. Biological control of *Acinetobacter baumannii*: In vitro and in vivo activity, limitations, and combination therapies. *Microorganisms*, **10**(5): 1-25.
- Hetta HF, Al-Kadmy IMS, Khazaal SS, Abbas S, Suhail A, El-Mokhtar MA, Ellah NHA, Ahmed EA, Abd-Ellatif RB, El-Masry EA, Batiha GE, Elkady AA, Mohamed NA and Algamal AM. 2021. Antibiofilm and antivirulence potential of silver nanoparticles against multidrug-resistant *Acinetobacter baumannii*. *Sci Rep*, **11**(1): 1-11.

- Ibrahim E, Fouad H, Zhang M, Zhang Y, Qiu W, Yan C, Li B, Mo J and Chen J. 2019. Biosynthesis of silver nanoparticles using endophytic bacteria and their role in inhibition of rice pathogenic bacteria and plant growth promotion. *RSC Adv*, **9(50)**: 1-7.
- Ibrahim S, Al-Saryi N, Al-Kadmy IMS and Aziz SN 2021. Multidrug-resistant *Acinetobacter baumannii* as an emerging concern in hospitals. *Mol Biol Rep*, **48(10)**: 1-11.
- Iravani S. 2014. Bacteria in nanoparticle synthesis: Current status and future prospects. *Int Sch Res Notices*, **2014**: 1-19.
- Kaur K, Reddy S, Barathe P, Shriram V, Anand U, Proćków J and Kumar V. 2021. Combating drug-resistant bacteria using photothermally active nanomaterials: A perspective review. *Front Microbiol*, **12**: 1-18.
- Khoshnood S, Eslami G, Hashemi A, Bahramian A, Heidary M, Yousefi Nojookambari N, Mohammadi F and Gholami M. 2017. Distribution of aminoglycoside resistance genes among *Acinetobacter baumannii* strains isolated from burn patients in tehran, iran. *Iran Arch Pediatr Infect Dis*, **5(3)**: 1-5.
- Kumar CG and Mamidyala SK. 2011. Extracellular synthesis of silver nanoparticles using culture supernatant of *pseudomonas aeruginosa*. *Colloids Surf B Biointerfaces*, **84(2)**: 462-466.
- Kumar G, Srivastava A and Singh R. 2020. Impact of nanoparticles on genetic integrity of buckwheat (*fagopyrum esculentum moench*). *Jordan J Biol Sci*, **13(1)**: 13-17.
- Laws M, Shaaban A and Rahman KM. 2019. Antibiotic resistance breakers: Current approaches and future directions. *FEMS Microbiol Rev*, **43(5)**: 490-516.
- Lee C-R, Lee JH, Park M, Park KS, Bae IK, Kim YB, Cha C-J, Jeong BC and Lee SH. 2017. Biology of *Acinetobacter baumannii*: Pathogenesis, antibiotic resistance mechanisms, and prospective treatment options. *Front Cell Infect Microbiol*, **7**: 1-35.
- Li YJ, Pan CZ, Fang CQ, Zhao ZX, Chen HL, Guo PH and Zhao ZW. 2017. Pneumonia caused by extensive drug-resistant *Acinetobacter baumannii* among hospitalized patients: Genetic relationships, risk factors and mortality. *BMC Infect Dis*, **17(1)**: 1-10.
- Limban C, Marutescu L and Chifiriuc MC. 2011. Synthesis, spectroscopic properties and antipathogenic activity of new thiourea derivatives. *Molecules*, **16(9)**: 7593-7607.
- Mancuso G, Midiri A, Gerace E and Biondo C. 2021. Bacterial antibiotic resistance: The most critical pathogens. *Pathogens*, **10(10)**: 1-14.
- Maspi H, Mahmoodzadeh Hosseini H, Amin M and Imani Fooladi AA. 2016. High prevalence of extensively drug-resistant and metallo beta-lactamase-producing clinical *Acinetobacter baumannii* in iran. *Microb Pathog*, **98**: 155-159.
- Mba IE and Nweze EI. 2021. Nanoparticles as therapeutic options for treating multidrug-resistant bacteria: Research progress, challenges, and prospects. *World J Microbiol Biotechnol*, **37(6)**: 1-30.
- Muhsin SS, Bakir WaE and Sabbah MA. 2022. Identification and sequencing of isaba2 of *Acinetobacter baumannii* isolated from baghdad hospitals. *Mustansiriyah Med J*, **21(1)**: 29-36.
- Nie D, Hu Y, Chen Z, Li M, Hou Z, Luo X, Mao X and Xue X. 2020. Outer membrane protein a (ompA) as a potential therapeutic target for *Acinetobacter baumannii* infection. *J of Biomed Sci*, **27(1)**: 1-8.
- Nirmala C and Sridevi M. 2021. Characterization, antimicrobial and antioxidant evaluation of biofabricated silver nanoparticles from endophytic *Pantoea anthophila*. *J Inorg Organomet Polym Mater*, **31(9)**: 3711-3725.
- Nji E, Kazibwe J, Hambridge T, Joko CA, Larbi AA, Dampthey LaO, Nkansa-Gyamfi NA, Stålsby Lundborg C and Lien LTQ. 2021. High prevalence of antibiotic resistance in commensal *Escherichia coli* from healthy human sources in community settings. *Sci Rep*, **11(1)**: 1-11.
- Oza G, Pandey DS, Shah R and Sharon M. 2012. Extracellular fabrication of silver nanoparticles using *Pseudomonas aeruginosa* and its antimicrobial assay. *Adv Appl Sci Res*, **3**: 1776-1783.
- Papenfort K and Bassler BL. 2016. Quorum sensing signal-response systems in gram-negative bacteria. *Nat Rev Microbiol*, **14(9)**: 576-588.
- Paul D and Sinha SN. 2014. Extracellular synthesis of silver nanoparticles using *Pseudomonas aeruginosa* kupsb12 and its antibacterial activity. *Jordan J Biol Sci*, **7(4)**: 245-250.
- Pavani K, Poojitha GS and Beulah M. 2020. Phytotoxicity of zinc-oxide nanoparticles on seedling growth and antioxidant activity of red gram (*Cajanus cajan* L.) seed. *Jordan J Biol Sci*, **13**: 153-158.
- Peiris MK, Gunasekara CP, Jayaweera PM, Arachchi ND and Fernando N. 2017. Biosynthesized silver nanoparticles: Are they effective antimicrobials? *Mem Inst Oswaldo Cruz, Rio de Janeiro*, **112**: 537-543.
- Peiris MMK, Fernando N, Jayaweera P, Hegoda Arachchi N and Gunasekara C. 2018. Comparison of antimicrobial properties of silver nanoparticles synthesized from selected bacteria. *Indian J Microbiol*, **58**: 1-11.
- Punjabi K, Yedurkar S, Doshi S, Deshapande S and Vaidya S. 2017. Biosynthesis of silver nanoparticles by *Pseudomonas* spp. Isolated from effluent of an electroplating industry. *IET Nanobiotechnol*, **11(5)**: 584-590.
- Raorane CJ, Lee JH and Lee J. 2020. Rapid killing and biofilm inhibition of multidrug-resistant *Acinetobacter baumannii* strains and other microbes by iodoindoles. *Biomolecules*, **10(8)**: 1-13.
- Saipriya K, Swathi CH, Ratnakar KS and Sritharan V. 2020. Quorum-sensing system in *Acinetobacter baumannii*: A potential target for new drug development. *J Appl Microbiol*, **128(1)**: 15-27.
- Shah S, Gaikwad S, Nagar S, Kulshrestha S, Vaidya V, Nawani N and Pawar S. 2019. Biofilm inhibition and anti-quorum sensing activity of phytosynthesized silver nanoparticles against the nosocomial pathogen *Pseudomonas aeruginosa*. *Biofouling*, **35(1)**: 34-49.
- Sherif MM, Elkhatib WF, Khalaf WS, Elleboudy NS & Abdelaziz NA. 2021. Multidrug resistant *Acinetobacter baumannii* biofilms: Evaluation of phenotypic–genotypic association and susceptibility to cinnamic and gallic acids. *Front Microbiol*, **12**: 1-15.
- Singh R, Shedbalkar UU, Wadhvani SA and Chopade BA. 2015. Bacteriogenic silver nanoparticles: Synthesis, mechanism, and applications. *Appl Microbiol Biotechnol*, **99(11)**: 4579-4593.
- Singh R, Vora J, Nadhe SB, Wadhvani SA, Shedbalkar UU and Chopade BA. 2018. Antibacterial activities of bacteriogenic silver nanoparticles against nosocomial *Acinetobacter baumannii*. *J Nanosci Nanotechnol*, **18(6)**: 3806-3815.
- Slavin YN, Ivanova K, Hoyo J, Perelshtein I, Owen G, Haegert A, Lin Y-Y, Lebiha S, Gedanken A, Häfeli UO, Tzanov T and Bach H. 2021. Novel lignin-capped silver nanoparticles against multidrug-resistant bacteria. *ACS Appl Mater Interfaces*, **13(19)**: 22098-22109.
- Sun X and Xiang J. 2021. Mechanism underlying the role of luxR family transcriptional regulator abar in biofilm formation by *Acinetobacter baumannii*. *Curr Microbiol*, **78(11)**: 3936-3944.
- Sunkar S and Nachiyar CV. 2012. Biogenesis of antibacterial silver nanoparticles using the endophytic bacterium *Bacillus cereus* isolated from *Garcinia xanthochymus*. *Asian Pac J Trop Biomed*, **2(12)**: 953-959.

Tang J, Chen Y, Wang X, Ding Y, Sun X and Ni Z. 2020. Contribution of the *abaI/abaR* quorum sensing system to resistance and virulence of *Acinetobacter baumannii* clinical strains. *Infect Drug Resist*, **13**: 4273-4281.

Tille PM. 2021. **Bailey & Scott's Diagnostic Microbiology**, 15th edition. Elsevier/Mosby, China.

Uddin TM, Chakraborty AJ, Khusro A, Zidan BMRM, Mitra S, Emran TB, Dhama K, Ripon MKH, Gajdács M, Sahibzada MUK, Hossain MJ and Koirala N. 2021. Antibiotic resistance in microbes: History, mechanisms, therapeutic strategies and future prospects. *J Infect Public Health*, **14(12)**: 1750-1766.

Urnuksaikhon E, Bold B-E, Gunbileg A, Sukhbaatar N and Mishig-Ochir T. 2021. Antibacterial activity and characteristics of silver nanoparticles biosynthesized from *carduus crispus*. *Sci Rep*, **11(1)**: 1-12.

Ventola CL. 2015. The antibiotic resistance crisis: Part 1: Causes and threats. *P T*, **40(4)**: 277-283.

Yang J, Wang Q, Wang C, Yang R, Ahmed M, Kumaran S, Velu P and Li B. 2020. *Pseudomonas aeruginosa* synthesized silver nanoparticles inhibit cell proliferation and induce *ros* mediated apoptosis in thyroid cancer cell line (tpc1). *Artif Cells Nanomed Biotechnol*, **48(1)**: 800-809.

Zhong S and He S. 2021. Quorum sensing inhibition or quenching in *Acinetobacter baumannii*: The novel therapeutic strategies for new drug development. *Front Microbiol*, **12**: 1-7.